VILNIUS UNIVERSITY

Zenonas Vaitonis

THERMAL EFFECTS IN HIGH-POWER LIGHT-EMITTING DIODES

Summary of doctoral thesis
Technological Sciences, Materials Engineering (08T)

Vilnius 2011

The research has been carried out in 2007–2011 at the Department of Semiconductors of the Faculty of Physics and the Institute of Applied Research, Vilnius University.

Scientific supervisor:

Prof. habil. dr. Artūras Žukauskas (Vilnius University, Physical Sciences, Physics, 02P).

Consultant:

Prof. habil. dr. Stanislavas Sakalauskas (Vilnius University, Physical Sciences, Physics, 02P).

Council on Materials Engineering (Technological Sciences) at Vilnius University:

Chairman:

Prof. habil dr. Sigitas Tamulevičius (Kaunas University of Technology, Technological Sciences, Materials Engineering, 08T).

Members:

Dr. Ramūnas Aleksiejūnas (Vilnius University, Physical Sciences, Physics, 02P).

Dr. Renata Butkutė (Vilnius University, Technological Sciences, Materials Engineering, 08T).

Prof. habil. dr. Romanas Martavičius (Vilnius Gediminas University, Technological Sciences, Electrical and Electronic Engineering, 01T).

Dr. Rolandas Tomašiūnas (Vilnius University, Technological Sciences, Materials Engineering, 08T).

Opponents:

Dr. Vaidas Pačebutas (Centre for Physical Science and Technology, Technological Sciences, Materials Engineering, 08T).

Prof. habil dr. Linas Svilainis (Kaunas University of Technology, Technological Sciences, Electrical and Electronic Engineering, 01T).

The official defence of the doctoral thesis will be held in the public session of the Council at 3 p.m. on December 16, 2011 in the lecture room 212 at the Faculty of Physics, Vilnius University, Saulėtekio al. 9, bldg. III, LT-10222 Vilnius, Lithuania.

The summary of the doctoral thesis has been distributed on November ….. , 2011.

The thesis is available at Vilnius University library and at the library of Institute of Physics of Centre for Physical Sciences and Technology.

VILNIAUS UNIVERSITETAS

Zenonas Vaitonis

ŠILUMINIAI REIŠKINIAI DIDELĖS GALIOS ŠVIESTUKUOSE

Daktaro disertacijos santrauka
Technologijos mokslai, medžiagų inžinerija (08T)

Vilnius 2011

Disertacija rengta 2007–2011 metais Vilniaus universiteto Fizikos fakulteto Puslaidininkių fizikos katedroje ir Taikomųjų mokslų institute.

Mokslinis vadovas:

Prof. habil dr. Artūras Žukauskas (Vilniaus universitetas, fiziniai mokslai, fizika 02P).

Konsultantas:

Prof. habil dr. Stanislavas Sakalauskas (Vilniaus universitetas, fiziniai mokslai, fizika 02P).

Vilniaus universiteto Technologijos mokslų srities medžiagų inžinerijos mokslų krypties taryba:

Pirmininkas:

Prof. habil dr. Sigitas Tamulevičius (Kauno technologijos universitetas, technologijos mokslai, medžiagų inžinerija – 08T).

Nariai:

Dr. Ramūnas Aleksiejūnas (Vilniaus universitetas, fiziniai mokslai, fizika – 02P).

Dr. Renata Butkutė (Vilniaus universitetas, technologijos mokslai, medžiagų inžinerija – 08T).

Prof. habil dr. Romanas Martavičius (Vilniaus Gedimino technikos universitetas, technologijos mokslai, elektros ir elektronikos inžinerija – 01T).

Dr. Rolandas Tomašiūnas (Vilniaus universitetas, technologijos mokslai, medžiagų inžinerija – 08T).

Oponentai:

Dr. Vaidas Pačebutas (Fizinių ir technologinių mokslų centras, technologijų mokslai, medžiagų inžinerija – 08T).

Prof. habil dr. Linas Svilainis (Kauno technologijos universitetas, technologijos mokslai, elektros ir elektronikos inžinerija – 01T).

Disertacija bus oficialiai ginama viešame tarybos posėdyje 2011 m. gruodžio 16 dieną, 15 valandą Vilniaus universiteto Fizikos fakulteto 212 auditorijoje, Saulėtekio al. 9, III rūmai, LT-10222 Vilnius, Lietuva.

Disertacijos santrauka išsiuntinėta 2011 m. lapkričio ..... d.

Disertaciją galima peržiūrėti Vilniaus universiteto ir Fizinių mokslų ir technologijų centro Fizikos instituto bibliotekose.

Santrauka

Pagrindinis disertacijos tikslas buvo ištirti šiluminius reiškinius ir jų sukeltus elektrinių bei išėjimo charakteristikų pokyčius prekiniuose didelės galios šviestukuose.

Disertacija yra sudaryta iš penkių skyrių. Kiekvieno skyriaus pabaigoje yra pateikiamos išvados. Disertanto kartu su bendraautoriais išpublikuotų mokslinių straipsnių ir konferencijų pranešimų sąrašas pateikiamas darbo pabaigoje. Disertacijos skyriai, kuriuos rengiant panaudota straipsnių medžiaga, ir paveikslėliai šiuose skyriuose pažymėti su citavimo nuorodomis į pastarąjį sąrašą.

Pirmasis disertacijos skyrius, sudarytas iš keturių poskyrių, skirtas 6viestuk7 sandūros temperatūros nustatymo iš elektroliuminescencijos spektro didelių energijų šlaito metodo tyrimui ir jo taikymo sąlygų apibrėžimui. Pirmame poskyryje pateiktas eksperimento aprašymas, kuriame nurodyti tiriamų šviestukų tipai, naudota aparatūra ir tyrimo sąlygos. Antrame ir trečiame poskyriuose aprašomi, atitinkamai, AlGaInP ir InGaN šviestukų heterosandūrų temperatūros nustatymo iš elektroliuminescencijos spektrų, rezultatai. Patekti rezultatai parodo sandūros temperatūros nustatymo iš elektroliuminescencijos spektro didelių energijų šlaito metodo taikymo galimybes ir sąlygas. Taip pat, dėmesys yra skirtas skirtingų metodų palyginimui.

Antras skyrius yra skirtas puslaidininkinio lusto temperatūros dinamikos tyrimui, kai šviestukas yra valdomas impulso pločio ir impulsų pasikartojimo dažnio moduliacijos būdais. Po eksperimento metodinės medžiagos, antrame poskyryje pateikiami eksperimentiniai sandūros temperatūros dinamikos matavimo rezultatai esant dviems skirtingiems valdymo būdams. Trečiame poskyryje pasiūlomas teorinis modelis, aprašantis sandūros temperatūros kitimą. Eksperimentiškai nustatytas ir teorinio modelio pagalba paaiškintas impulsų dažnio moduliacijos taikymo šviestukų valdymui pranašumas dėl didesnio našumo ir pastovesnių išėjimo charakteristikų.

Trečiame skyriuje aprašomas detalus baltų konversijos fosforuose šviestukų spalvio priklausomybės nuo aplinkos temperatūros ir tiesioginės srovės tyrimas. Pirmame poskyryje pateikiama informacija apie tyrimo eigą. Antrame poskyryje aprašyti tyrimo rezultatai ir pasiūlytas paprastas spalvio kitimo skaitinis modelis, kuris sėkmingai gali būti panaudotas prekinių puslaidininkinių šviestukų techniniame aprašyme. Pagal šį

modelį apskaičiuotas spalvis nedaug skiriasi nuo eksperimentinių rezultatų, o skirtumas gali būti mažesnis už spalvio suvokimo ribą visame temperatūrų ir srovių intervale.

Ketvirtas skyrius yra skirtas šiluminiam ir nešiluminiam poveikiui elektroliuminescencijos moduliacijos spektrui esant harmoninei šviestukų tiesioginės srovės moduliacijai. Šiame skyriuje aprašytas tyrimas, kurio metu buvo nustatyti įvairių AlGaInP ir InGaN šviestukų elektroliuminescencijos harmoninės moduliacijos gylio spektrai. Gauti rezultatai atskleidė sandūros temperatūrai jautrias spektro sritis. Ištyrus temperatūrai jautrių sričių moduliacijos gylio priklausomybę nuo moduliacijos dažnio, buvo nustatytos šviestuką sudarančių konstrukcijos elementų šiluminės relaksacijos trukmės.

Penktajame disertacijos skyriuje pateikiamas šviestukų elektrinių charakteristikų kitimas, jiems senstant darbinėmis šiluminėmis sąlygomis. Čia aprašomas sendinimo metu nustatytas tiesioginės įtampos, nuosekliosios varžos ir krūvininkų injekcijos proceso charakteringosios energijos mažėjimas. Gauti rezultatai buvo paaiškinti ilgalaikio iškaitinimo darbinėje temperatūroje sukelta Mg–H kompleksų disociacija, dėl kurios padidėja jonizuotų priemaišų tankis šviestuko p apvalkaliniame sluoksnyje.

Acknowledgement

I would like to thank my scientific supervisor prof. Artūras Žukauskas for expressed trust and provided help in the preparation of my doctoral thesis.

I express many thanks to the consultant Prof. Stanislavas Sakalauskas for the helpful scientific discussions and consultations.

Additionally I wish to thank all co-authors of the joint publications for the productive collaboration in performing research as well as in preparing papers and conference contributions.

Introduction

Artificial light is being used by humans for ages following the progress in the development of light sources. The most advanced lighting technology is based on light-emitting diodes (LEDs), which are already widely used in general and special illumination [1]. The phenomenon of electroluminescence (EL), which is the principle of operation of LEDs, has been discovered in the beginning of the XX^{th} century [2], although this phenomenon was explained by radiative recombination of free carriers much latter [3]. A huge progress in solid-state lighting was attained after the adapting of metalorganic chemical vapour deposition (MOCVD) technology for the growth of high-quality AlGaInP and InGaN semiconductor layers by the end of the XX^{th} century [4,5]. By using heterostructures based on these semiconductors, light can be efficiently generated within a wide range of chromaticities.

Radiant efficiency of about 50% and luminous efficiency in excess of 200 lm/W have already been achieved for direct-emission coloured LEDs and phosphor converted white LEDs, respectively [6,7]. However, high output fluxes are attained while operating LEDs in severe driving conditions (1 to 10 W electrical power), which result in an increase of junction temperature due to the selfheating effect. The junction temperature is an important parameter that influences all characteristics of a LED. An increased junction temperature results in the alteration of electrical characteristics, such as forward voltage and series resistance. Also, the efficiency, as well as the peak wavelength, bandwidth, chromaticity, and frequency response of EL are sensitive to the selfheating effect due to the sensitivity of the rate of radiative and nonradiative recombination, band gap energy, carrier distribution function, and phosphor photoluminescence to temperature.

The measurement of junction temperature usually is based on the temperature sensitivity of a LED parameter. A well established approach is the forward-voltage method [8]. Alternatively, the junction temperature can be determined remotely from the high-energy wing of the EL spectrum. However, a disparity in the values of junction temperature measured using different methods was revealed [9]. Therefore, a detailed investigation of the latter method should be performed.

The junction temperature of a LED oscillates under pulsed driving. The character of such oscillation depends on the duration and repetition frequency of the forward-current pulses and on the thermal response of the LED chip, which contains components with different thermal relaxation constants. As the result, the output characteristics of the LED might be different at different driving modes. This poses a problem of the selection of a driving mode that is optimal in terms of the thermal regime and might be different form the commonly used pulse-width modulation mode.

White LEDs have a polychromatic spectral power distribution that is composed of both direct-emission EL band and/or photoluminescence bands due to the conversion of EL in phosphors [10]. Therefore, the dependence of white LED chromaticity on forward current and ambient temperature is intricate and difficult to describe using analytical models. To that end, numerical models with an appropriate accuracy are of high interest.

The oscillation of junction temperature can influence the modulation properties of LEDs. However, the thermal and athermal effects on the frequency response of LEDs and on the spectral distribution of modulation depth are rarely reported in literature and deserve more attention.

The selfheating of LED chip might result in the alteration of electrical characteristics during long-term operation. Although LED aging effects received considerable attention [11], the long-term variation of the electrical characteristics of LEDs is to be addressed in more detail.

Keeping in mind the issues mentioned above, the thesis was aimed at the investigation of steady-state and transient thermal effects in high-power LEDs. The **main goals** of this work were the investigation of different thermal characterization methods, thermal response of LEDs, and the dependence of electrical and output characteristics on junction temperature.

Main objectives

To validate the method of LED junction temperature measurement from the high-energy wing of the EL spectrum. To investigate the possibility of the application of this method and to compare it with another ones.

To compare the pulse-width modulation and pulse-frequency modulation driving modes in terms of the transient behaviour of junction temperature and output characteristics.

To investigate the dependence of white LED chromaticity on ambient temperature and forward voltage and to introduce a simple numerical model for the simulation of chromaticity coordinates with perceptually acceptable accuracy.

To investigate the EL modulation spectrum of high-power LEDs and to elucidate the effect of junction temperature oscillation in different parts of the spectrum.

To investigate the variation of electrical characteristics of commercial InGaN LEDs during long-term aging under rated thermal condition.

Novelty and significance of the thesis

The method of LED junction temperature measurement from the high-energy wing of the EL spectrum has been validated and compared to other methods.

A comparison of the pulse-width modulation and pulse-frequency modulation driving modes in terms of junction temperature oscillation and output characteristics of a high-power LED has been performed.

A simple numerical model for the simulation of chromaticity coordinates of white LEDs as a function of ambient temperature and forward current has been proposed.

The spectral distribution of modulation depth of EL has been investigated in high-power AlInGaP and InGaN LEDs and explained in terms of thermal and athermal effects. The thermal characterization of the LEDs was performed using the sensitivity of particular parts of the modulation spectrum to junction temperature oscillation.

The alteration of electrical characteristics of InGaN LEDs during long-term aging has been investigated. The results were proposed to attribute to long-term annealing under rated thermal conditions.

Points to be maintained (statements to defence)

1. The junction temperature of AlGaInP light-emitting diodes, which emit due to the recombination of free carriers, can be determined directly from the high-energy wing of electroluminescence spectrum. Calibration measurements should be carried out for the measurement of junction temperature in InGaN light-emitting diodes, which emit is due to the recombination of localized carriers.
2. In comparison with the pulse-width modulation driving mode, the pulse-frequency modulation driving mode is advantageous in a higher efficiency, steadier chromaticity and lower junction temperature oscillation.
3. The chromaticity coordinates of phosphor conversion white light-emitting diodes can be numerically simulated within acceptable tolerance (3 MacAdam ellipses) as flat functions of ambient temperature and forward current.
4. The spectral distribution of electroluminescence modulation is uneven in AlGaInP light-emitting diodes driven by harmonically modulated forward current due to the thermal modulation of band gap and free carrier distribution function. The spectral distribution of electroluminescence modulation in InGaN light-emitting diodes is due only to the thermal modulation of delocalized carrier distribution function. Different parts of the electroluminescence spectrum have different sensitivity to junction temperature oscillation.
5. The forward voltage, series resistance and characteristic energy of carrier injection decrease during long-term aging of high-power InGaN light-emitting diodes under rated thermal conditions.

1. Measurement of LED junction temperature from the high-energy slope of the EL band [P1]

An important parameter in operating LEDs is the junction temperature, which conditions the efficiency, chromaticity, and longevity of a device. The measurement of LED junction temperature rely on numerous techniques, among which the most established are the methods of forward voltage [8] and EL band peak position [9]. The main drawback of these methods is the necessity of individual calibration of each LED prior to examination. Alternatively, the junction temperature can be determined directly from the high-energy slope of the EL spectrum, which reflects the distribution function of nonequilibrium carriers in the active layer of a LED. The short-wavelength wing of the EL band can be quantified by the inverse derivative T_{ID} of logarithmic intensity with respect to photon energy $h\nu$ and expressed in temperature units

$$T_{\mathrm{ID}}(\Delta)=\left[-k_{\mathrm{B}}\frac{\partial(\ln I)}{\partial(h\nu)}\bigg|_{\Delta}\right]^{-1}, \tag{1.1}$$

where I is the spectral intensity of EL, $\Delta = h\nu - E_{\mathrm{P}}$ is the distance from peak position (E_{P} is the peak position of the EL band). However, the values of LED junction temperature measured using different methods exhibit a disparity [9]. In this work, the high-energy slope method for the measurement of the junction temperature of high-power AlGaInP and InGaN LEDs has been validated.

High-power (1 W) red AlGaInP (Philips Lumileds Lighting model LXHL-MD1R) and blue InGaN (Philips Lumileds Lighting model LXHL-MRRD) LEDs were studied.

AlGaInP LEDs emit due to the band-to-band recombination of free carriers in the bulk-like active layer, which is about 1 μm in thickness. For tree-dimensional statistics, the shape of the EL band can de expressed as

$$r(h\nu)=Ah\nu\,\mathrm{Re}\sqrt{h\nu-E_{\mathrm{g}}}\,\exp\left(-\frac{h\nu}{k_{\mathrm{B}}T_{\mathrm{c}}}\right), \tag{1.2}$$

were A is a constant, E_{g} is the energy gap, T_{c} is the temperature of carriers. The carrier temperature, which is assumed to equal junction temperature, can be estimated from the experimental inverse derivative T_{ID} as the characteristic temperature T_{S}, obtained form the differentiation of Eq. (1.2):

$$T_{\mathrm{S}} = \frac{\Delta}{k_{\mathrm{B}}}\left[\sqrt{1+\frac{2k_{\mathrm{B}}T_{\mathrm{ID}}(\Delta)}{\Delta}}-1\right]. \qquad (1.3)$$

Figure 1.1 shows characteristic temperature as a function of distance from the peak position in the AlGaInP LED measured in the self-heating-free (pulsed) regime for various chip temperatures and driving currents. The range from 90 meV to 150 meV (gray area in Fig. 1.1) is seen to accurately reflect the actual junction temperature (dashed horizontal lines). Moreover, the independence of characteristic temperature on forward current was observed. Meanwhile, the characteristic temperature decreases at photon energies higher than 150 meV from the peak position due probably to photon absorption in cladding layers.

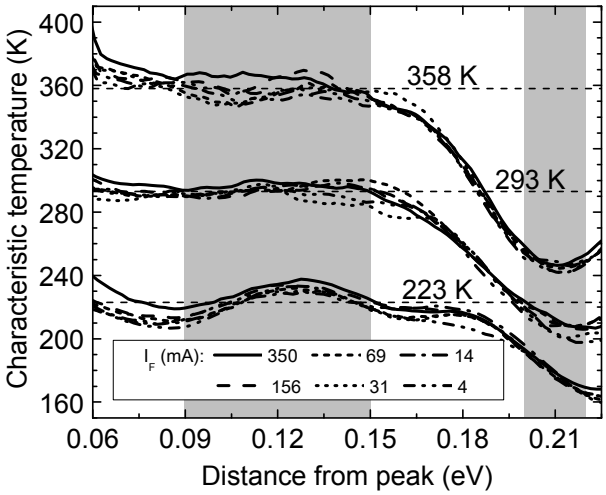

Fig. 1.1. Characteristic temperature derived from the high-energy wing of the EL spectra for a high-power red AlGaInP LED as a function of distance from the EL band peak for various driving currents. The dashed horizontal lines demarcate chip temperature (indicated) [P1].

The junction temperature calibration curves of the red AlGaInP LED are shown in Fig. 1.2. A linear function $T_{\mathrm{J}} = mT_{\mathrm{S}} + T^*$ was used for the approximation of the calibration data. The approximation parameter $m = 1$ and a small temperature bias $T^* = -6$ K were determined for characteristic temperature determined in the 90 meV to 150 meV spectral interval. This means that the junction temperature can be accurately determined directly from

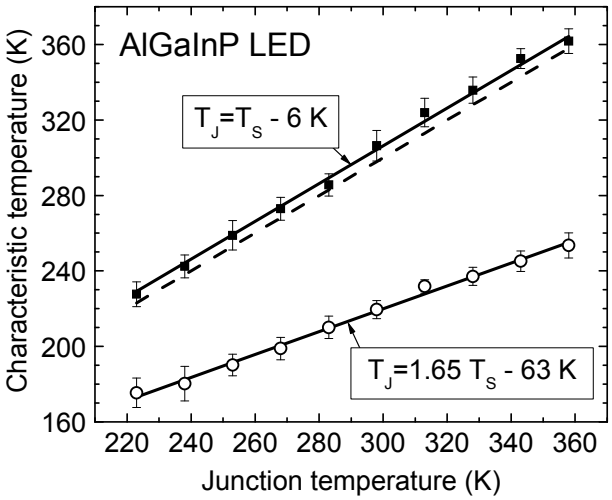

Fig. 1.2. Calibration charts for the measurement of junction temperature in a red AlGaInP LED obtained from the inverse derivative of the high-energy wing of the EL spectra at the rated current. The filled squares are the characteristic temperature in the transparent spectral window; open circles are those in the reabsorbed spectral window. The solid lines are linear approximations as indicated and the dashed line is the equality dependence $T_{\mathrm{J}} = T_{\mathrm{S}}$ [P1].

characteristic temperature. Meanwhile, the characteristic temperature measured in the range of 150 meV above the peak position noticeably deviates from junction temperature. For instance in the range from 200 meV to 220 meV corresponding to EL reabsorption, the approximation parameters are $m = 1.65$ and $T^* = -63$ K. This means that calibration measurements should be performed for junction temperature measurement in this interval.

For the validation of high-energy slope method, a comparison of junction temperature determined from the high-energy wing of the EL spectrum with that measured by the forward-voltage method was performed. The estimated difference in junction temperature was found to not exceed 3 K (1%) for the transparent spectral window. For the spectral window corresponding to the reabsorbed high-energy wing, the difference amounts up to 18 K (5%–7%).

InGaN LEDs contain a multiple-quantum-well active layer with carriers subjected to quantum confinement and described within two-dimensional statistics, which should result in a simple high-energy exponential slope ($T_{ID} = T_c$). However, the effect of localized carriers (excitons) that dominate the emission results in that the actual shape of the high-energy wing of the EL spectra in InGaN LEDs is more complex and is determined by the Gaussian distribution of the localized states and inhomogeneous broadening.

The inverse derivatives of the EL spectra of the InGaN LED as a function of distance form the EL band peak are shown in Fig. 1.3. With increasing the distance, the inverse derivative is seen to approach the actual junction temperature. However, it does not reach junction temperature due to broadening and the distortion of the EL spectra in cladding layers. In the spectral range from 140 meV to 160 meV above the peak position, the junction temperature can be estimated using an appropriate

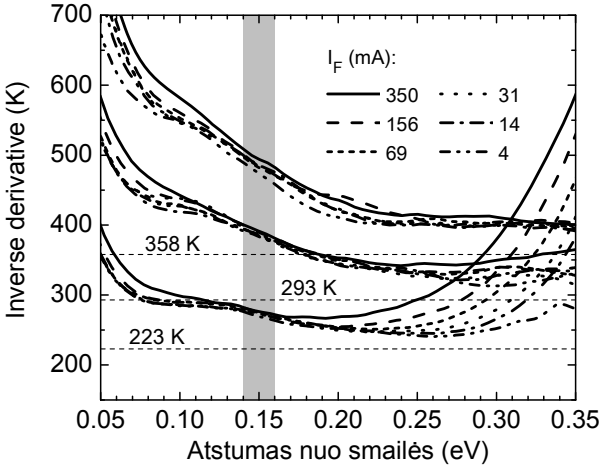

Fig. 1.3. Inverse derivative of the high-energy wing for a high-power blue InGaN LED as a function of the distance from the peak for various driving currents. The dashed horizontal lines demarcate chip temperature (indicated) [P1].

correction procedure. For instance, a linear function $T_J = mT_{ID} + T^*$ with $m = 0.66$ and $T^* = 43$ K can be used in this spectral interval. The calibration chart for the measurement of junction temperature from inverse derivative in the selected spectral window is shown in Fig. 1.4 at two values of forward current.

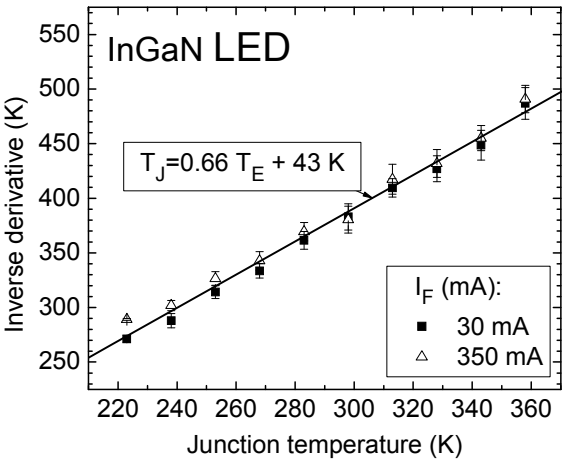

Fig. 1.4. Calibration chart for the measurement of junction temperature in a blue InGaN LED obtained from the inverse derivative of the high-energy wing of the EL spectra at two forward currents. The solid line is a linear approximation as indicated [P1].

Summary

In AlGaInP LEDs, which contain a thick active layer, the junction temperature can be directly measured with an accuracy of about 2 % as the characteristic temperature obtained from the inverse derivative of the spectra with the 3D density of states taken into account. The spectral region for such a measurement must be free from parasitic absorption.

In InGaN LEDs, extraction of junction temperature from the inverse derivative of the EL spectra is aggravated by a complex effect of thermal broadening on the shape of localized-carrier EL band and by an admixture of free carrier emission. Nevertheless, the inverse derivative at about 150 meV above the peak energy can be linearly linked to junction temperature by using a correction factor and bias term.

2. Dynamics of the junction temperature of LEDs under pulsed driving [P5]

The control of LED output can be performed using different methods of driving. The pulse-width modulation (PWM) driving mode is frequently used instead of the constant current regulation (CCR) mode due to the simplicity of driving electronics and steadier output characteristics [12,13]. However, the oscillation of junction temperature caused by the pulsed driving results in the variation of output flux parameters within the pulse repetition period. One can anticipate that the use of shorter current pulses makes the oscillations of junction temperature, output flux, and chromaticity of a LED smaller. To

that end, comparison of the PWM and pulse-frequency modulation (PFM) driving modes was performed in this part of the work.

A high-power (1 W) amber AlGaInP LED (Philips Lumileds Lighting model LXHL-ML1D) was used for the investigation of the driving methods. The driving pulses of the rated forward current (350 mA) with the duration varied from 200 μs to 20 m at a constant repetition frequency of 50 Hz were used in PWM driving mode. Meanwhile, a constant pulse duration of 200 μs with the pulse repetition frequency varied from 50 Hz to 5 kHz was used in the PFM dimming mode. The CCR driving method was also used for comparison.

The junction temperature was traced within the entire pulse repetition period using the forward-voltage method [8]. (In order to measure the junction temperature during the "off" phase, a small bias current of 3.5 mA was applied.) The dynamics of junction temperature under pulsed driving at a duty cycle of 50 % and for three different pulse repetition frequencies is shown in Fig. 2.1 (circles). It can be seen, that the magnitude of junction temperature oscillation is decreased at a higher pulse repetition frequency. However, the average junction temperature remains constant. For comparison of PWM and PFM driving modes, the output characteristics were investigated. The points in Fig. 2.2 (a) correspond to the time-integrated intensity of EL at the PFM (circles), PWM (squeres) and CCR (triangles) dimming modes. The dash-dotted line indicates hypothetical intensity without the self-heating effect. The deviation of time-integrated intensity from self-heating free intensity is shown in Fig. 2.2 (b) by points. The deviation is the same for all driving

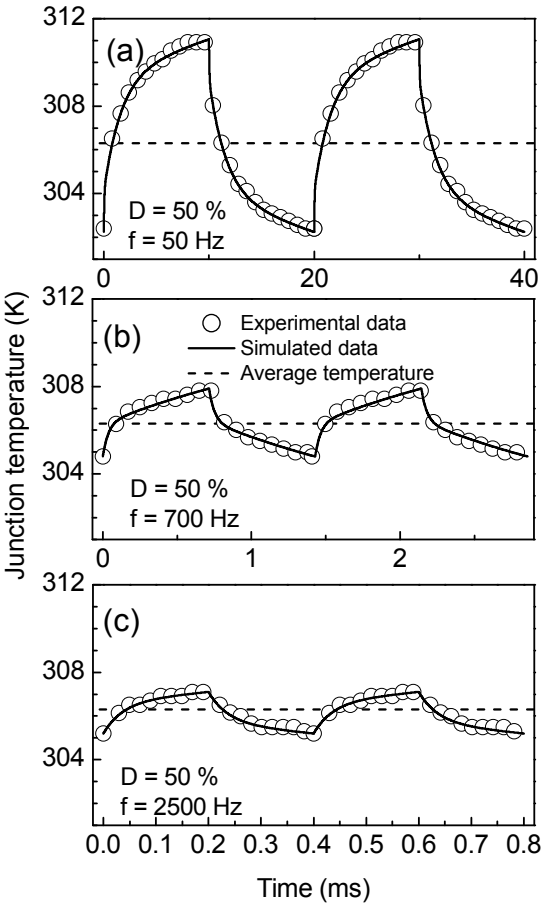

Fig. 2.1. Transients of the junction temperature of an amber AlGaInP LED driven at different pulse repetition rates. Points, data measured using the forward-voltage method; solid lines, reconstruction using the proposed model; dashed line, the average junction temperature [P5].

modes at the duty cycle of 100 %. However, the difference in deviation was observed at decreased duty cycles. The smallest deviation was found for the CCR driving mode. Meanwhile, the PFM method showed better results than the PWM. The efficiency of LED is by 5 % higher for the PFM dimming at a duty cycle 50 %. Also, a linear dependence of deviation was observed for the PFM driving method, which makes the compensation of self-heating effect easier.

Figure 2.3 (a) shows the peak wavelength dependence on duty cycle. A linear increase of peak wavelength up to 2.6 nm was observed with increasing duty cycle for the CCR driving mode. The variation of peak wavelength for the PWM and PFM dimming methods is not linear. However, the deviation from linearity is very small for the PFM mode. The parts (b) and (c) of Fig. 2.3 depict the dependences of chromaticity coordinates on duty cycle. Again, the variation of chromaticity coordinates is almost linear in the CCR dimming mode and deviates from linearity in the pulsed driving modes. However, the deviation from a linear dependence in the PFM mode is much smaller than that in the PWM mode.

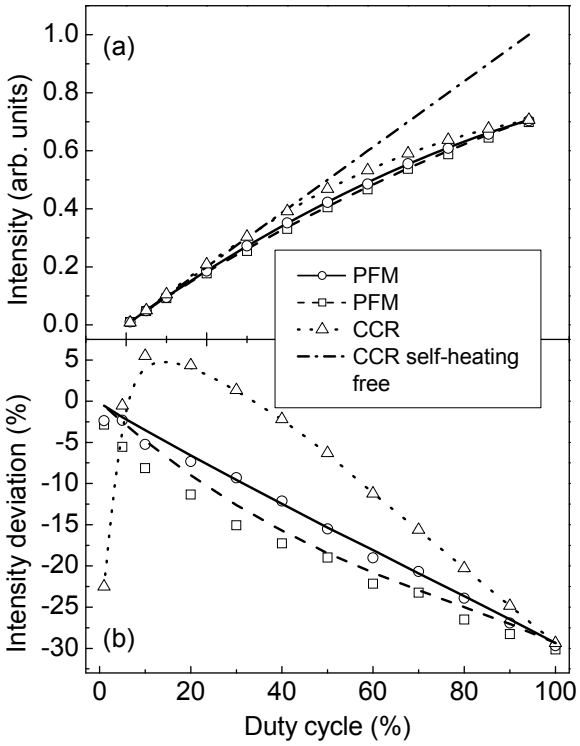

Fig. 2.2. Time-integrated intensity and deviation of intensity from the self-heating-free output characteristic as functions of duty cycle for the three driving modes. The solid and dashed lines show the results of simulation using the model [P5].

A simple model was proposed for the explanation of the experimental data on the oscillation of junction temperature. The minimal junction temperature equals ambient temperature T_A, and the maximal temperature can be calculated using the thermal resistance of LED, R_θ,

$$T_{J\max} = T_A + R_\theta\left(V_F I_F - \Phi\right), \tag{2.1}$$

where V_F is the forward voltage, I_F is the forward current, and Φ is the optical power.

The variation of junction temperature with time during one period can be expressed as

$$T_{\mathrm{J}} = \begin{cases} T_{\mathrm{J}}(0) + \left[T_{\mathrm{J\,max}} - T_{\mathrm{J}}(0)\right]\left[1 - \sum_i \alpha_i \exp\left(-\dfrac{t}{\tau_i}\right)\right] & \text{for } 0 \le t \le t_{\mathrm{p}}, \\ T_{\mathrm{A}} + \left[T_{\mathrm{J}}(t_{\mathrm{p}}) - T_{\mathrm{A}}\right]\sum_i \alpha_i \exp\left(-\dfrac{t - t_{\mathrm{p}}}{\tau_i}\right) & \text{for } t_{\mathrm{p}} \le t \le t_0; \end{cases} \tag{2.2}$$

where $T_{\mathrm{J}}(0)$ is the junction temperature at the beginning of the period, t_{p} is the duration of the current pulse, t_0 is the period, and α_{i} and τ_{i} are the fractional contributions and the time constants of the i-th thermal relaxation path, respectively.

The lines in Fig. 2.1 show the reconstructed transient behaviour of the junction temperature of the amber LED for $T_{\mathrm{A}} = 295$ K, $R_\theta = 20$ K/W and three-exponential thermal response function with the time constants of $\tau_1 = 37$ μs, $\tau_2 = 1.6$ ms and $\tau_3 = 0.54$ s. The shortest time constant can be assigned to the heat flow from the junction to the bottom cladding layer of the chip. The second one can be assigned to heat relaxation through the metal base of the chip. The longest time constant corresponds to heat dissipation in the remaining parts of the LED and external heat sink.

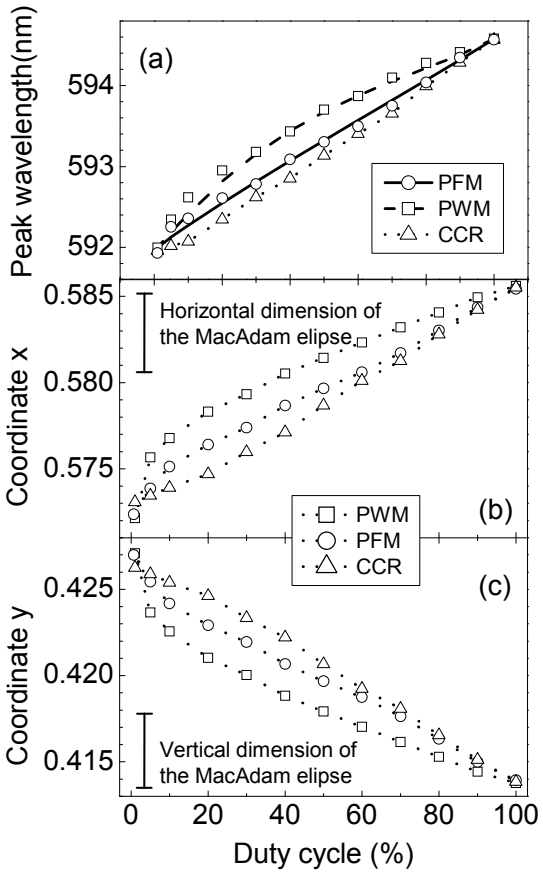

Fig. 2.3. Peak position and chromaticity coordinates of EL as functions of duty cycle. Solid and dashed lines, the results of simulation using the model [P5].

The above results show that the output characteristics of a LED driven by repetitive current pulses depend on the driving mode. A gain in efficiency of about 5 % at a duty cycle of 50 % can be achieved for the LED investigated under the PFM driving mode due to reduced junction temperature oscillation. Another advantage of the PFM driving mode with respect to the PWM one is the almost linear dependences of output intensity

deviation from the self-heating-free dependence, peak position and chromaticity coordinates on duty cycle.

Summary

Using a time-resolved forward-voltage method, the oscillation of the junction temperature of a LED driven by repetitive current pulses was studied within a wide range of pulse widths and repetition frequencies. The measured transients of junction temperature can be quantitatively described by a simple model that is based on a multi-exponent thermal response function. The thermal-relaxation model was shown to account for the output characteristics measured in the PFM and PWM driving modes. An increased efficiency and higher steadiness of output characteristics is the benefit of the PFM driving mode.

3. Numerical model of the chromaticity of white LEDs dependence on ambient temperature and forward current

The chromaticity of phosphor converted white LEDs depends on temperature and forward current. This feature should be taken into account in applications that are sensitive to colour quality of illumination. The chromaticity varies due to several reasons as follows [12,13]. The shape of the EL spectrum of the InGaN chip depends on junction temperature and forward current. Meanwhile, the intensity of phosphor photoluminescence decreases, the width of spectral line broadens and the peak position shifts to longer wavelength due to phosphor heating. Usually, LED datasheets lack information on the variation of the chromaticity of emitted light.

In this work, the chromaticity of white LEDs was investigated as a function of two variables, ambient temperature and forward current, and a simple numerical model for simulating chromaticity coordinates was proposed.

High power (1 W) phosphor converted white LEDs (Philips Lumileds Lighting) were studied. Three warm white LEDs (model LXHL-MWGC, correlated colour temperature 3500 K) and three neutral white LEDs (model LXHL-MW1D, correlated colour temperature 5000 K) were studied. The ambient temperature and forward current of the LEDs were varied within wide ranges. The grids of chromaticity coordinates at

different operation conditions are shown in Fig. 3.1. Figures 3.1 (a) and (b) correspond to the surfaces of CIE x and y chromaticity coordinates, respectively, for warm white LEDs. Figures 3.1 (c) and (d) show similar data for neutral white LEDs. The surfaces of chromaticity coordinates are seen to be non-flat. However, we propose a simple model for simulating the x and y coordinates dependence on ambient temperature and forward current. The experimental data were fitted by the planes, which are described as

$$x(I_{\mathrm{F}}, T_{\mathrm{A}}) = x_0 + a + b \cdot \frac{I_{\mathrm{F}} - I_{\mathrm{F0}}}{I_{\mathrm{F0}}} + c \cdot \frac{T_{\mathrm{A}} - T_{\mathrm{A0}}}{T_{\mathrm{A0}}} \tag{3.1}$$

and

$$y(I_{\mathrm{F}}, T_{\mathrm{A}}) = y_0 + d + e \cdot \frac{I_{\mathrm{F}} - I_{\mathrm{F0}}}{I_{\mathrm{F0}}} + f \cdot \frac{T_{\mathrm{A}} - T_{\mathrm{A0}}}{T_{\mathrm{A0}}}, \tag{3.2}$$

were x_0 and y_0 are the CIE chromaticity coordinates of a LED at rated conditions (T_{A0} = 20 °C, I_{F0} = 350 mA), and a, b, c, d, e and f are the model parameters.

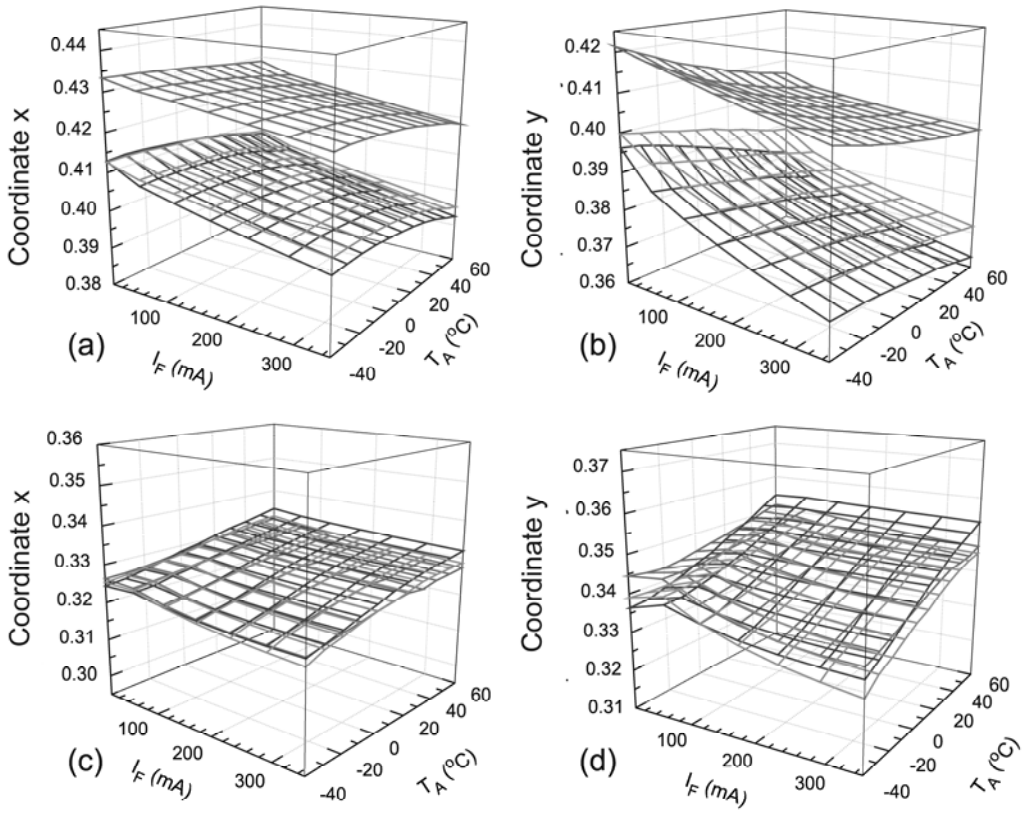

Fig. 3.1. CIE chromaticity coordinates x and y of the white high-power LEDs as functions of ambient temperature and forward current. Parts (a) and (b), warm white LEDs; parts (c) and (d), neutral white LEDs.

The interpolated MacAdam ellipses [14] were used for the validation of the model. The perceived difference in chromaticity was considered as significant when it is larger than the dimension of the ellipse *M* (distance from the centre to the edge of the ellipse) multiplied by a factor of 3. Two methods for choosing the parameters in Eqs. (3.1) and (3.2) were applied. The less square method yields chromaticity planes that are positioned closer to the most data. Meanwhile at the edges of the experimental chromaticity surfaces, the deviation from the modelled planes is high. Therefore, we applied a least-deviation method for modelling the chromaticity planes. The application of this method gives smaller misalignment of the experimental surfaces with the model planes.

The parameters of the proposed model were optimized for every LED separately. For the unification of the model, the average values of the parameters were calculated for two types of devices. Then, a numerical simulation of chromaticity coordinates and correlated colour temperature were performed for each LED using the average values. The largest deviation of calculated chromaticity from the measured one was 3.03*M* for the least-deviation model. The largest deviation of correlated colour temperature was 150 K. Meanwhile, the largest deviation of calculated chromaticity from the measured one was 3.14*M* for the least-square method.

Figure 3.2 shows an example of the simulation of chromaticity coordinates using the two different methods.

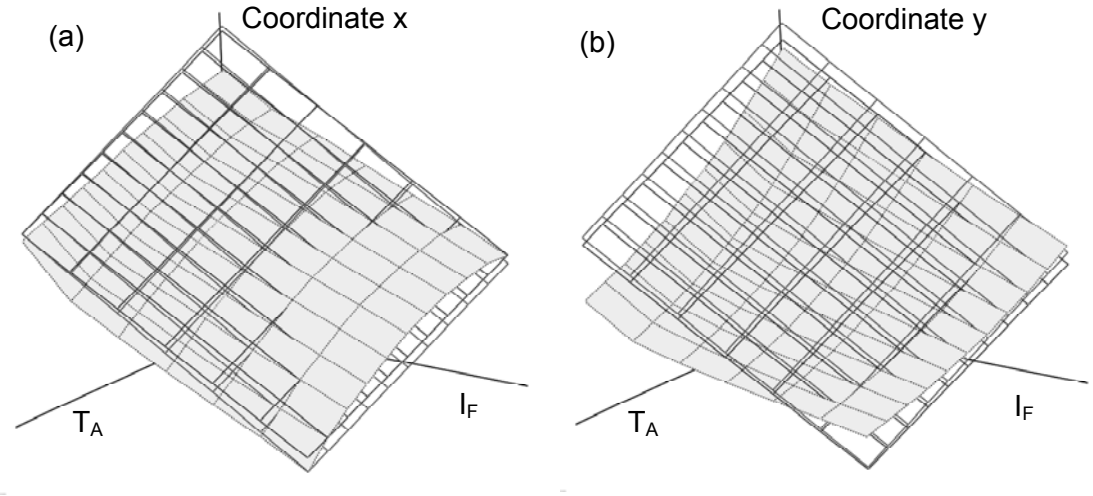

Fig. 3.2. Chromaticity coordinates *x* (a) and *y* (b) of a white LED as functions of ambient temperature and forward current. Gray surface, experimental data; gridded planes, the chromaticities simulated using the two different methods.

Summary

The surfaces of the chromaticity coordinates as functions of ambient temperature and forward current were determined. A flat approximation of the experimental data was proposed and the parameters of two different numerical methods were found. The model of least chromaticity deviation shows a better match of the experimental and simulated data that the least-square model. The modelled chromaticities deviate from the experimental ones within 3-step MacAdam ellipses, which is the perceptually acceptable tolerance.

4. Thermal and athermal effects on EL spectral modulation of LEDs [P3–P4]

LEDs are compact and easy to modulate sources of light, which are used in spectroscopy and communication for years. However, the spectral dependence of EL modulation, which might be important in wavelength-division-multiplexed optical networks [15], optical sensors [16], and intelligent signalling and lighting systems [17], has not been revealed so far. Such dependence can be influenced by the oscillation of junction temperature caused by modulated driving.

In this part of the thesis, the EL modulation spectra were studied in high-power LEDs and thermal and athermal effects on these spectra were revealed. Commercial high-power AlGaInP and InGaN LEDs (Philips Lumileds Lighting, LXHL series) were investigated. The red, red-orange and amber AlGaInP LEDs feature a double heterojunction with a bulk-like active layer emitting due to the band-to-band recombination of free carriers. The blue and green InGaN LEDs have a multiple-quantum-well active layer emitting due mainly to carriers localized at the band potential minima of the alloy.

Figures 4.1 (a), (b) and (c) show the EL spectra of red, red-orange, and amber LEDs, respectively, at a constant forward current of 350 mA. The EL modulation spectra of the LEDs driven by forward current with a bias of 350 mA and modulation depth of 5 % are shown in Figs. 4.1 (b), (d) and (f), respectively. The common features of the spectra for the red and red-orange LEDs are as follows: i) a constant increase in modulation depth in the low-energy wing of the EL spectrum; ii) a dip at a photon energy near the peak position; and iii) a linear increase of modulation depth with photon energy in the high-

energy wing of the EL spectrum. At a high modulation frequency, which us above the thermal cut-off frequency, these features are smoother and, probably, are caused by athermal broadening of the EL spectrum. The amber LED differs from other AlGaInP diodes in that no increase of modulation in the high-energy wing of the EL spectrum is observed due to the effect of EL reabsorption in the GaP window layer. The solid and doted horizontal lines in Fig. 4.1 represent the modulation depth of spectrally integrated EL above the thermal cut-of frequency and at zero frequency.

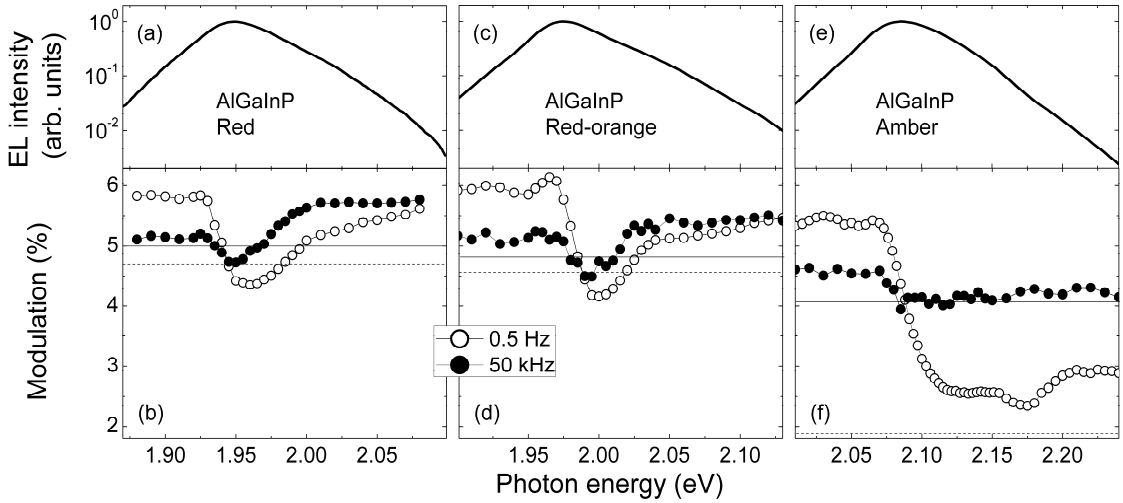

Fig. 4.1. EL spectra of high-power red (a), red-orange (c) and amber (e) AlGaInP LEDs at a constant forward current of 350 mA. Parts (b), (d) and (f), EL modulation spectra of the same LEDs at high and low modulation frequencies [P3–P4].

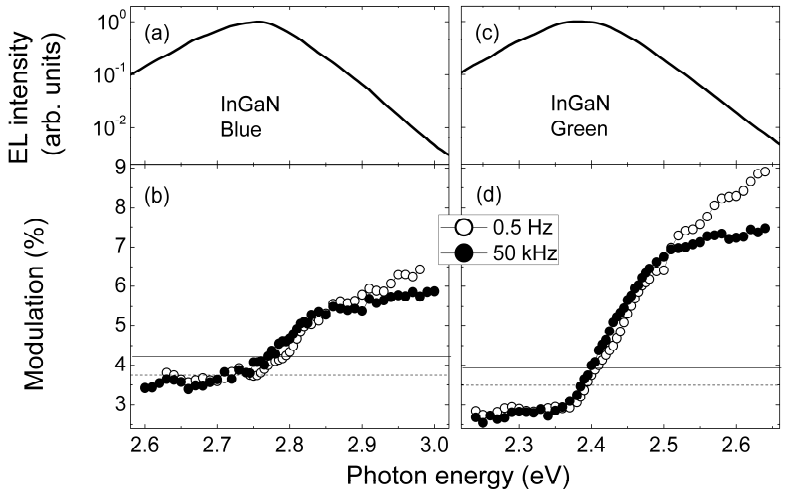

Fig. 4.2. EL spectra of high-power blue (a) and green (c) InGaN LEDs at a constant forward current of 350 mA. (b) and (d) EL modulation spectra of the same LEDs at high and low modulation frequencies [P3–P4].

Figures 4.2 (a) and (c) show the EL spectra of the blue and green InGaN LEDs, respectively. Figures 4.2 (b) and (d) display the corresponding EL modulation spectra. The modulation spectra of the InGaN LEDs have no dip near the EL spectrum peak position and the modulation depth in the low-energy wing is lower than that at the peak. In these parts of the spectrum, the modulation depth does not depend on frequency as is to be attributed to an athermal effect. However, in the far high-energy region, the slope of the EL modulation spectra is sensitive to frequency, i.e. it is influenced by junction temperature oscillation.

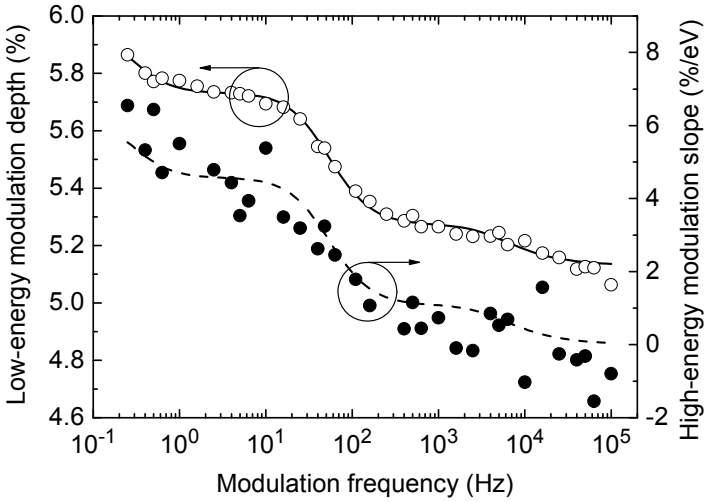

Fig. 4.3. Dependences of modulation depth in the low-energy wing (open points) and the slope of the modulation spectrum in the high-energy wing of the EL spectrum (filled points) on modulation frequency in the red LED. Solid and dashed lines, fitting to a three-component thermal frequency response function [P3–P4].

The comparison of the EL modulation spectra at low and high modulation frequencies revealed the spectral regions that have a high sensitivity to the oscillation of junction temperature. In AlGaInP LEDs, the most sensitive feature is the modulation depth in the low-energy wing of the EL spectrum. Meanwhile, in InGaN LEDs, the most sensitive feature is the slope of modulation spectrum in the far high-energy region. Figure 4.3 shows the measured frequency dependences of EL modulation depth in the low-energy wing and the slope of the EL modulation spectrum in high-energy wing in the red AlGaInP LED. Figure 4.4

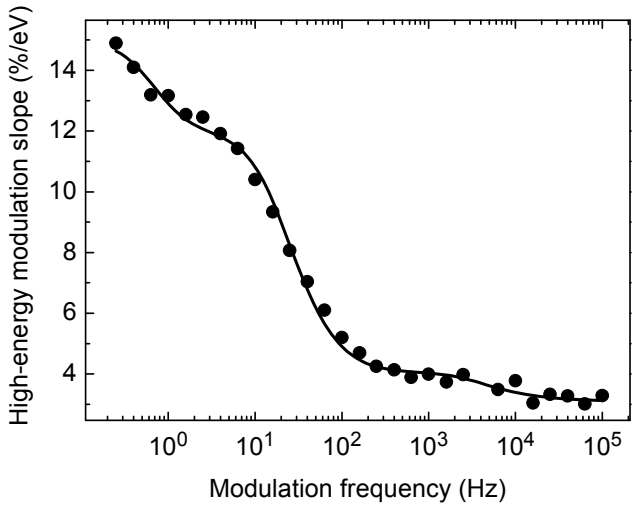

Fig. 4.4. Points, dependence of the slope of the modulation spectrum in the high-energy wing of the EL spectrum on modulation frequency in the green LED. Solid line, fitting to a three-component thermal frequency response function [P3–P4].

shows the frequency dependence of the slope in the green InGaN LED. The observed step-like experimental dependences were fitted to thermal frequency response functions containing several thermal relaxation time constants.

The best fit for the red LED was obtained for a three-component thermal frequency response function with thermal relaxation time constants $\tau_1 = 37$ μs, $\tau_2 = 4.0$ ms and $\tau_3 = 0.58$ s, respectively. A similar response function with thermal relaxation time constants $\tau_1 = 50$ μs, $\tau_2 = 9.0$ ms and $\tau_3 = 0.25$ s, respectively, was used for the green LED. These time constants correspond to thermal dissipation through different parts of the LEDs.

In order to account for the spectral features of EL modulation spectra of the LEDs, a model, which considers junction temperature oscillation due to transient self-heating, was introduced. The excess junction temperature oscillates around the mean value T_0 under harmonically modulated driving as

$$T(t) - T_\mathrm{A} = (T_0 - T_\mathrm{A})[1 + m_T(\omega)\sin\{\omega t - \varphi_T(\omega)\}]; \tag{4.1}$$

where T_A is the ambient (heat sink) temperature, m_T is the junction temperature modulation depth, ω is the angular frequency of forward current modulation, φ_T is the phase shift between the current and junction temperature waveforms. Meanwhile for modulated forward current and junction temperature, the spectrally integrated flux oscillates around the mean value Φ_0, with the modulation depth m_Φ and phase shift φ_Φ,

$$\Phi(t) = \Phi_0(1 + m_\Phi(\omega)\sin[\omega t - \varphi_\Phi(\omega)]). \tag{4.2}$$

The analysis of the EL spectral modulation based on Eqs. (4.1) and (4.2) with a glance to the EL spectral power distribution of the LEDs yielded the analytical expressions of modulation depth in different parts of the spectrum.

The spectral modulation depth in the low-energy wing of the EL spectrum of AlGaInP LEDs, which emit due to free-carrier recombination, can be presented as

$$m_{\Phi\mathrm{L}}(\omega) \approx m_\Phi(\omega) - \frac{T_0 - T_\mathrm{A}}{E_0}\frac{\partial E_\mathrm{g}}{\partial T} m_T(\omega)\cos\varphi_T(\omega), \tag{4.3}$$

where E_0 is the characteristic energy of the low-energy slope of the EL spectrum, which is assumed to weakly depend on temperature and current and $\partial E_\mathrm{g}/\partial T$ is the temperature

coefficient of band gap energy. The dip of the modulation spectrum is located at the photon energy

$$h\nu_{\min} \approx E_{\mathrm{g}} + k_{\mathrm{B}} T_0 \sqrt{-\frac{1}{2k_{\mathrm{B}}} \frac{\partial E_{\mathrm{g}}}{\partial T}} \tag{4.4}$$

and the modulation depth at the dip is

$$m_{\min}(\omega) \approx m_{\Phi}(\omega) - \left(\frac{3}{2} - \frac{1}{k_{\mathrm{B}}} \frac{\partial E_{\mathrm{g}}}{\partial T} \right) \frac{T_0 - T_{\mathrm{A}}}{T_0} m_T(\omega) \cos \varphi_T(\omega). \tag{4.5}$$

In the high-energy limit, the modulation depth increases linearly with photon energy due to the thermal modulation of the carrier distribution function. The corresponding slope is

$$\frac{\partial m_{\Phi \mathrm{H}}(\omega, h\nu)}{\partial h\nu} \approx \frac{T_0 - T_{\mathrm{A}}}{T_0} \frac{m_T(\omega)}{k_{\mathrm{B}} T_0} \cos \varphi_T(\omega). \tag{4.6}$$

The multiple-quantum well active layer of high-power InGaN LEDs emits due to carriers localized at the band potential minima of the alloy. The red shift of the EL due to the thermal effect on band gap energy counteracts the blue shift due to the band filling effect [18]. Therefore, one might expect that the drop of modulation depth around the EL peak photon energy is less prominent than that defined by Eqs. (4.4) and (4.5) and that the low-energy modulation depth is smaller than that defined by Eq. (4.3).

In an InGaN LED, the EL spectrum above the peak photon energy can be presented as

$$\Phi_{\mathrm{H}}(I_{\mathrm{F}}, T, h\nu) \propto \Phi(I_{\mathrm{F}}, T) \exp\left[-\frac{h\nu - E_{\mathrm{g}}(T)}{k_{\mathrm{B}}\left(a \cdot T - T^*\right)} \right], \tag{4.7}$$

where a and T^* are the constants, that can by obtained from a calibration measurement. Therefore, the thermal modulation of the carrier distribution function results in an increase of modulation depth with photon energy far above the band gap energy as

$$\frac{\partial m_{\Phi \mathrm{H}}(\omega, h\nu)}{\partial h\nu} \approx \frac{T_0 - T_{\mathrm{A}}}{k_{\mathrm{B}}\left(aT_0 + T^*\right)^2} m_T(\omega). \tag{4.8}$$

In AlGaInP LEDs, our model of the EL modulation spectrum explains the low-frequency experimental data by junction temperature oscillation in all three spectral

regions (low-energy, peak, and high-energy). Meanwhile in InGaN LEDs, the spectral variation of modulation depth is mainly due to athermal effects and the transient self-heating manifests itself only in the far high-energy region of the spectrum.

Summary

The EL modulation spectra of high-power AlGaInP and InGaN LEDs were studied. The effect of junction temperature oscillation on the EL modulation spectrum was revealed by measuring the spectrum at two modulation frequencies, below and above the thermal cut-off frequency, respectively. In the red and red-orange AlGaInP LEDs, the modulation spectrum exhibits the features as follows: i) a dip at the photon energy somewhat above the EL peak photon energy; ii) an almost photon-energy-independent modulation enhancement in the low energy wing of the EL spectrum; and iii) a linear increase of modulation depth with photon energy in the high-energy wing of the EL spectrum. These features were found to be in a quantitative agreement with a theoretical model proposed.

In the blue and green InGaN LEDs, the effect of junction temperature oscillation on EL spectral modulation was revealed only in the far high-energy region of the spectra, where the emission is strongly contributed by the band-to-band recombination of free carriers. Meanwhile, almost no effect of transient self-heating was observed in the low energy and central regions of the EL spectrum. Such a result was attributed to thermal redistribution of localized carriers over the band-tail states, which compensates the thermal narrowing of band gap.

5. Aging effect on electrical characteristics of LEDs [P2]

Advanced LEDs feature longevity and high efficiency in comparison to other light sources. However for solid lighting systems designed for long-term operation, the alteration of electrical characteristics within the operating time can occur and must be predicted. Commonly, the following changes of LED electrical characteristics are observed: i) an increase of forward current due to an increase of the rate of nonradiative recombination; ii) an increase of reverse current; iii) a decrease of forward current at the rated voltage due to the deterioration of the electrical contact between the chip and

electrodes [11]. In this part of the work, the effect of long-term aging under rated thermal conditions on electrical characteristics in high-power InGaN LEDs was investigated.

Four high-power blue InGaN LEDs (Philips Lumileds Lighting, model LXHL-MRRD) were under study. The aging experiment was conducted under rated conditions. The series resistance and conductivity of the heterojunction were determined from the *I-V* characteristics measured within a wide range of forward currents. To avoid ambiguities due to short-term aging effects, the first measurements of electrical characteristics were performed after 500 hours of seasoning.

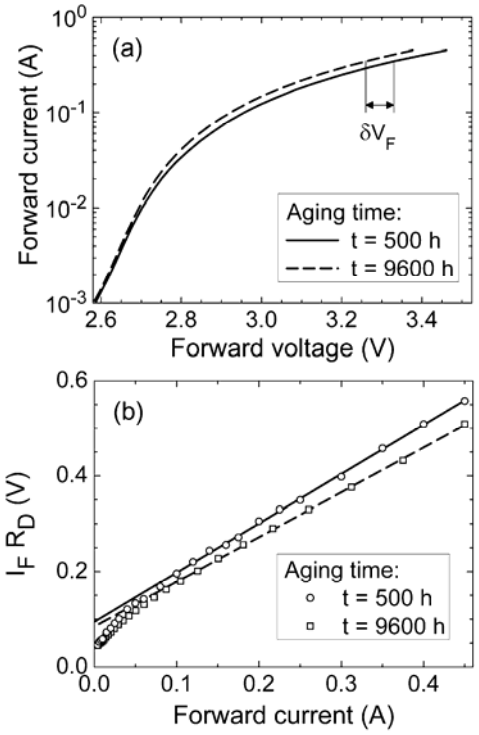

Fig. 5.1. (a) Semilogarithmic and (b) differential *I-V* characteristics of a high-power InGaN LED just after 500-h seasoning and after 9600-h aging [P2].

Figure 5.1 shows the typical *I-V* characteristics of a LED just after 500-h seasoning and after 9600-h aging. Only marginal difference of forward current in just opened LED can be seen. However, a significant difference in forward voltage ($\delta V_F \approx -70$ mV) was observed at the rated current of 350 mA. Such variation corresponds to a decrease of series resistance of the LED.

The observed alteration of the *I-V* characteristics was analyzed in terms of the Shockley equation for diffusion, recombination and tunnel injection mechanisms, which are typical of InGaN LEDs

$$I_F = \sum_i I_{0i} \left\{ \exp\left[\frac{V_F - I_F R_S}{E_i / q} \right] - 1 \right\}, \tag{5.1}$$

where I_{0i} and E_i are the reverse saturation current and the energy parameter of the i-th injection process, respectively, R_S is the series resistance, q is the elementary charge. Assuming that the injection current is dominated by a single component on the right-

hand side of Eq. (5.1) and $I_F >> I_0$, differentiation by forward current yields the dynamic resistance

$$R_D \equiv \frac{dV_F}{dI_F} = R_S + \frac{E_0}{qI_F}. \tag{5.2}$$

The second term on the right-hand side of Eq. (5.2) is the inverse junction conductivity, which for a particular forward current is determined by solely the energy parameter of the injection process. To distinguish between the components of the dynamic resistance, the differential *I-V* characteristics, which is obtained from Eq. (5.2), can by used

$$I_F R_D \equiv I_F \frac{dV_F}{dI_F} = I_F R_S + \frac{E_0}{q}. \tag{5.3}$$

By plotting the product $I_F R_D$ as a function of forward current, both the series resistance (the slope) and the characteristic injection energy (the extrapolated value at $I_F = 0$) can be extracted.

Figure 5.1 (b) shows the differential *I-V* characteristics just after seasoning and after long-term aging. The slope of the curves corresponds to serial resistances of (1,032±0,025) Ω and (0,938±0,025) Ω, respectively. Meanwhile, the extrapolation revealed the values of characteristic energy (94±5) meV and (85±5) meV just after seasoning and after 9600 hours, respectively.

Figure 5.2 displays the cumulative results of the effect of aging on electrical parameters of four high-power InGaN LEDs at the nominal current. The decrease of forward voltage with a rate of 6,7 mV/1000 h or 0,2 %/1000 h, the

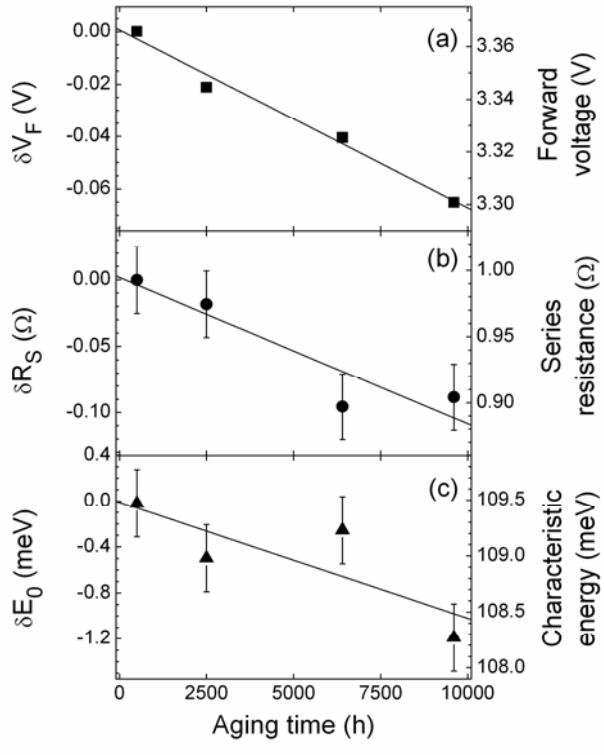

Fig. 5.2. Average variation of the electrical parameters of four high-power InGaN light-emitting diodes with time: (a) forward voltage at nominal current, (b) series resistance, (c) characteristic energy of the injection process [P2].

decrease of series resistance with a rate of ~0,011 Ω/1000 h or 1,1 %/1000 h and the decrease of characteristic energy of injection mechanism with a rate of ~0,1 meV/1000 h or 0.09 %/1000 h were determined from the figure.

A detailed analysis revealed at least two comparable contributions of the aging effect, a decrease in series resistance and a decrease in characteristic energy. The decrease in series resistance could be attributed to continuous annealing of the p cladding layer in the light-emitting structure. Such a post-fabrication self-annealing can result in a higher density of holes due to the dissociation of residual Mg–H complexes. Normally, the nominal junction temperature is too low to invoke the breakdown of the Mg–H bonds, which are known to dissociate at about 1000 K. However, in forward-biased diodes, minority-carrier-enhanced debonding of hydrogen is known to facilitate annealing at much lower temperatures [19]. Under assumption of an exponential probability of dissociation with an activation energy of about 1 eV on the minute scale, one can expect a similar annealing effect at 350 K on the 1000-hour scale.

The increase of junction conductivity probably has a more complex origin due to both the variation of the density of ionized acceptors in the p cladding layer and the density of localized states in the active layers.

Summary

We observed a long-term decrease of forward voltage in high-power InGaN LEDs and applied an analytical approach for *I-V* characteristics that revealed the variation of series resistance and junction conductivity with aging time. The decrease of series resistance was attributed to slow post-fabrication self-annealing of the p-type cladding layer facilitated by minority carriers under the rated thermal conditions.

References

[1] A. Žukauskas, M. S. Shur, and R. Gaska, *Introduction to Solid-State Lighting* (Wiley, New York, 2002).

[2] H. J. Round, Electrical World **49**, 309 (1907).

[3] K. Lehovec, C. A. Accardo, and E. Jamgochian, Phys. Rev. **83**, 603 (1951).

[4] C. H. Chen, S. A. Stockman, M. J. Peansky, and C. P. Kuo, in *High Brightness Light Emitting Diodes*, ed. by G. B. Stringfellow and M. G. Craford (Academic Press, New York, 1997), pp. 97–148.

[5] S. Nakamura and G. Fasol, *The Blue Laser Diode: GaN Based Light Emitters and Lasers* (Springer, Berlin, 1997).

[6] M. R. Krames, M. Ochiai-Holcomb, G. E. Höfler, C. Carter-Coman, E. I. Chen, I.-H. Tan, P. Grillot, N. F. Gardner, H. C. Chui, J.-W. Huang, S. A. Stockman, F. A. Kish, M. G. Craford, T. S. Tan, C. P. Kocot, M. Hueschen, J. Posselt, B. Loh, G. Sasser, and D. Collins, Appl. Phys. Lett. **75**, 2365 (1999).

[7] M. R. Krames, O. B. Shchekin, R. Mueller-Mach, G. O. Mueller, L. Zhou, G. Harbers, and M. G. Craford, J. Display Technol. **3**, 160 (2007).

[8] Y. Xi and E. F. Schubert, Appl. Phys. Lett. **85**, 2163 (2004).

[9] Y. Xi, J.-Q. Xi, T. Gessmann, J. M. Shah, J. K. Kim, E. F. Schubert, A. J. Fischer, M. H. Crawford, K. H. A. Bogart, and A. A. Allerman, Appl. Phys. Lett. **86**, 031907 (2005).

[10] M. S. Shur and A. Žukauskas, Proc. IEEE **93**, 1691 (2005).

[11] M. Meneghini, S. Podda, A. Morelli, R. Pintus, L. Trevisanello, G. Meneghesso, M. Vanzi, and E. Zanoni, Microelectron. Reliab. **46**, 1720 (2006).

[12] M. Dyble, N. Narendran, A. Bierman, and T. Klein, Proc. SPIE **5941**, 59411H (2005).

[13] Y. Gu, N. Narendran, T. Dong, and H. Wu, Proc. SPIE **6337**, 63370J (2006).

[14] A. Žukauskas, R. Vaicekauskas, F. Ivanauskas, H. Vaitkevičius, P. Vitta, and M. S. Shur, IEEE J. Sel. Top. Quantum Electron. **15**, 1753 (2009).

[15] M. H. Reeve, A. R. Hunwicks, W. Zhao, S. G. Methley, L. Bickers, and S. Hornung, Electron. Lett. **24**, 389 (1988).

[16] G. Murtaza and J. M. Senior, IEEE Photonics Technol. Lett. **6**, 1020 (1994).

[17] G. Pang, T. Kwan, H. Liu, and C.-H. Chan, IEEE Industry Appl. Mag. **8**, 21 (2002).

[18] T. Mukai, M. Yamada, and S. Nakamura, Jpn. J. Appl. Phys. **37**, L1358 (1998).

[19] S. J. Pearton, J. W. Lee, and C. Yuan, Appl. Phys. Lett. **68**, 2690 (1996).

List of publications related to the thesis

Papers

P1. **Z. Vaitonis**, P. Vitta, and A. Žukauskas, "Measurement of the junction temperature in high-power LEDs from the high-energy wing of the electroluminescence band," J. Appl. Phys. **103**(9), 093110, 7 p. (2008).

P2. **Z. Vaitonis**, A. Miasojedovas, A. Novičkovas, S. Sakalauskas, and A. Žukauskas, "Effect of long-term aging on series resistance and junction conductivity of high-power InGaN LEDs," Lith. J. Phys. **49**(1), pp. 69–74 (2009).

P3. **Z. Vaitonis**, P. Vitta, V. Jakštas, and A. Žukauskas, "Thermal effects on spectral modulation properties of high-power LEDs," Proc. SPIE **8120**, 812016, 11 p. (2011).

P4. **Z. Vaitonis**, P. Vitta, V. Jakštas, and A. Žukauskas, "Self-heating and athermal effects on the electroluminescence spectral modulation of an AlGaInP LED," J. Appl. Phys. **110**, 073103, 7 p. (2011).

P5. **Z. Vaitonis**, A. Stonkus, and A. Žukauskas, "Effect of junction temperature on output characteristics of a LED under pulse-width and pulse-frequency modulation driving modes," IET Optoelectron., *accepted*.

Conference contributions

K1. A. Miasojedovas, **Z. Vaitonis**, „Senėjimo įtaka didelės galios šviesos diodų elektrinėms charakteristikoms", Studentų mokslinė konferencija „Laisvieji skaitymai 2008". Programa ir pranešimų tezės (Vilnius, 2008 m. balandžio 4 d.), p. 67.

K2. **Z. Vaitonis** and A. Miasojedovas, "Electrical characteristics of LEDs dependence on long-term aging process," 10th Int. Conf.-School "Advanced Materials and Technologies." Abstracts (Palanga, Lithuania, August 27–31, 2008), p. 141.

K3. P. Vitta, **Z. Vaitonis**, and A. Žukauskas, "Measurement of the junction temperature in high-power LEDs from the high-energy wing of the electroluminescence band," 10th Int. Conf.-School "Advanced Materials and Technologies." Abstracts (Palanga, Lithuania, August 27–31, 2008), p. 44, *Best poster award.*

K4. **Z. Vaitonis**, P. Vitta, and A. Žukauskas, "Measurement of the junction temperature in high-power LEDs from the high-energy wing of the electroluminescence band," Int. Workshop Nitride Semicond. IWN 2008. Abstracts (Montreux, Switzerland, October 6–10, 2008), p. 501.

K5. A. Stonkus, **Z. Vaitonis**, A. Žukauskas, „Šviesos diodų spalvinių charakteristikų tyrimas esant impulsiniam maitinimui", 38-oji Lietuvos nacionalinė fizikos konferencija. Programa ir pranešimų tezės (Vilnius, 2009 m. birželio 8–10 d.), p. 260.

K6. P. Vitta, **Z. Vaitonis**, A. Žukauskas, „Puslaidininkinių šviestukų šiluminis charakterizavimas", 38-oji Lietuvos nacionalinė fizikos konferencija. Programa ir pranešimų tezės (Vilnius, 2009 m. birželio 8–10 d.), p. 264.

K7. P. Vitta, **Z. Vaitonis**, and A. Žukauskas, "Thermal characterization of LEDs," XXXVIII Int. School on the Phys. of Semiconducting Compounds Jaszowiec 2008. Abstracts (Ustrón-Jaszowiec, Poland, June 19–26, 2009), p. 63.

K8. **Z. Vaitonis**, A. Stonkus, and A. Žukauskas, "Thermal and colour characteristics of high-power LEDs under pulsed driving," 11th Int. Conf.-School „Advanced materials and Technologies". Abstracts (Palanga, Lithuania, August 27–31, 2009), p. 94.

K9. A. Stonkus and **Z. Vaitonis**, "Thermal and chromaticity characterization of high-power LEDs under pulsed driving", Studentų mokslinė konferencija „Laisvieji skaitymai 2010". Tezės (Vilnius, 2010 m. kovo 24 d.), p. 90.

K10. A. Žukauskas, **Z. Vaitonis**, and A. Stonkus, "Output characteristics of LEDs under different modes of pulsed driving," 7th Int. New Exploratory Technol. Conf. Proc. NEXT 2010 (Turku, Finland, October 19–21, 2010), p. 87.

K11. **Z. Vaitonis**, V. Jakštas, P. Vitta, and A. Žukauskas, "Spectral modulation of LEDs," 13th Int. Conf.-School "Advanced Materials and Technologies". Abstracts (Palanga, Lithuania, August 27–31, 2011), pp. 70.

K12. **Z. Vaitonis**, P. Vitta, V. Jakštas, and A. Žukauskas, "Thermal effects on spectral modulation properties of high-power LEDs," Photonic Fiber and Crystal Devices: Advances in Materials and Innovations in Device Applications V. SPIE Optics+Photonics 2011, Photonic Devices+Applications, Technical Summaries (San Diego, August 21–22, 2011), p. 99.

K13. **Z. Vaitonis**, R. Vaicekauskas, A. Žukauskas, „Baltų šviestukų spalvio priklausomybe nuo temperatūros ir tiesioginės srovės modelis“,39-ji Lietuvos nacionalinė fizikos konferencija. Programa ir pranešimų tezės (Vilnius, 2011 m. spalio 6–8 d.), p. 28.

List of papers not included into the thesis

N1. S. Sakalauskas and **Z. Vaitonis**, “Dynamic C-V characteristics of MOS structure,” Lith. J. Phys. **47**(4), pp. 451–456 (2007).

N2. S. Sakalauskas, **Z. Vaitonis**, and R. Pūras, “A linearly variable high-voltage amplifier,” Instrim. Exp. Tech. **50**(3), pp. 340–342 (2007).

N3. S. Sakalauskas, **Z. Vaitonis**, R. Pūras, and V. Bulbenkienė, “High speed C-V converter,” Elektron. Elektrotech. **6**, pp. 73–76 (2008).

N4. I. Buchovec, **Z. Vaitonis**, and Ž. Lukšienė, “Novel approach to control Salmonella enterica by modern biophotonic technology: photosensitization,” J. Appl. Microbiol **106**(3), pp. 748–754 (2009).

N5. **Z. Vaitonis** and Ž. Lukšienė, “LED-based light sources for decontamination of food: modeling photosensitization-based inactivation of pathogenic bacteria,” Lith. J. Phys., **50**(1), pp. 141–145 (2010).

N6. S. Sakalauskas, **Z. Vaitonis**, and R. Pūras, “A high-speed capacitance-to-voltage converter,” Instrum. Exp. Tech. **54**(5), pp. 692–694 (2011).

Information about the author

Name and surname:	Zenonas Vaitonis	
Birth date and place:	February 2, 1983, Kupiškis, Lithuania	
E-mail:	zenonas.vaitonis@gmail.com	
Education:	2001	12^{th} secondary school of Panevėžys
	2005	Bachelor Degree in Physics, Vilnius University
	2007	Master Degree in Physics, Vilnius University
	2007–2011	Doctoral studies at Vilnius University
Scientific experience:	2004–till now	Junior scientific researcher at the Institute of Applied research, Vilnius University
Specialization:	Application of LEDs in measurements and solid-state lighting systems. Optical, electrical and thermal characterization of LEDs.	
Publications:	Co-author of 11 papers listed in Thomson Reuters ISI WOS^{SM}.	